THE ASTROPHYSICAL JOURNAL, 303:25–38, 1986 April 1

ALIGNMENT OF CLUSTERS AND GALAXIES ON SCALES UP TO 0.1c

R. BRENT TULLY
Institute for Astronomy, University of Hawaii
Received 1985 April 4; accepted 1985 October 1

ABSTRACT

Three remarkable properties of the large-scale distribution of galaxies appear to have escaped attention: (1) The structure in the vicinity of the Virgo Cluster that has traditionally been called the Local Supercluster seems to be appended to a *very large agglomeration* that includes the Coma/A1367, Hydra-Centaurus, Perseus-Pisces, and Pisces-Cetus Superclusters. The whole entity includes 48 known Abell-class clusters, 10^{17}–10^{18} $M_\odot$, and extends across a diameter of 360 h_{75}^{-1} Mpc $\approx 0.09c$. (2) This very large structure is flattened, with axial ratios 4:2:1; and the pole, defined by the orientation of the short axis, is *coincident with the pole of the plane of the traditional Local Supercluster* to within 10°. (3) Within 40 h_{75}^{-1} Mpc of our location, where we have reasonable completion, there is a suggestion that the distribution of galaxies is *stratified* into four layers. Within a radius of 0.1c there are two other very large superclusters and many voids.

Subject headings: cosmology — galaxies: clustering

I. SUPERGALACTIC COORDINATES

There is an evident concentration of the brightest 1000 galaxies into a great circle on the sky. Nearby galaxies congregate in a plane centered on the Virgo Cluster. This structure is referred to as the Local Supercluster (de Vaucouleurs 1953, 1956, and many more recent publications, e.g., 1975; Tully 1982). The plane of the Local Supercluster defines the equatorial plane of a spherical coordinate system (SGL, SGB, distance: de Vaucouleurs and de Vaucouleurs 1964; de Vaucouleurs, de Vaucouleurs, and Corwin 1976).[1]

In this article, it is pointed out that there are other entities aligned with the supergalactic equator that are independent of the objects that led to the definition of supergalactic coordinates and that span a remarkably large range of scales. On a scale of order tens of megaparsecs, almost all nearby clouds of galaxies lie in planes parallel to the principal plane described above. All of this nearby structure is embedded in structure on a scale of several hundred megaparsecs that lies in the same plane.

II. STRATIFICATION OF NEARBY STRUCTURE

Within 40 h_{75}^{-1} Mpc, there are three prominent secondary layers parallel to the main plane of the Local Supercluster. These layers are evident in Figure 1, which is a smoothed histogram of the distribution of galaxies as a function of distance from the supergalactic equator.[2] The "raw" plot already includes a correction for incompletion as a function of distance. The "normalized" plot is adjusted for the decrease in unobscured area within the boundary of the sample as a function of distance from the main plane.[3]

The very prominent equatorial feature in Figure 1 is made up of a large number of subcondensations that extend across the entire Northern Galactic Hemisphere within 3000 km s^{-1} and must be presumed to continue to larger distances. Some of the most prominent subcondensations are the Virgo, Virgo W, and Ursa Major Clusters, the Virgo Southern Extension, and our home in the Canes Venatici Cloud. This flattened, broken-up structure has a long dimension in excess of 80 h_{75}^{-1} Mpc and a short dimension of roughly 4 h_{75}^{-1} Mpc.

The feature in Figure 1 that is 13 h_{75}^{-1} Mpc north of the supergalactic equator contains four condensations: the Virgo III Cloud (Tully 1982), the NGC 5371 Group and surroundings, and clouds in Pegasus and rising out of Grus. The feature 8 h_{75}^{-1} Mpc south of the supergalactic equator contains the Southern Supercluster around Fornax (de Vaucouleurs 1956) and the Leo II and Crater Clouds (Tully 1982) and, if the sample volume were to be extended only 10% further, would include the rich Centaurus Cluster. At 23 h_{75}^{-1} Mpc south of the supergalactic equator there is a chain of galaxies associated with the Antlia Cluster, and just beyond the sample volume in this plane lies Hydra I.

A detailed description of the structure in the distribution of nearby galaxies is beyond the scope of this article. An attempt will be made to do that in the *Atlas of Nearby Galaxies* (Tully and Fisher 1986). It will be seen there that the vast majority of galaxies within 40 h_{75}^{-1} Mpc lie in the features that have just been identified. In all but two cases, *these features are thin normal to the supergalactic equator*. For the Virgo III and Pegasus Clouds at high supergalactic latitudes, the principal plane, the Southern Supercluster and Leo II and Crater Clouds below it, and the Antlia region below these, in each case the long dimension is several tens of megaparsecs and the SGZ dimensions is typically 5 h_{75}^{-1} Mpc. In only two cases, the NGC

[1] A Cartesian system can be defined such that the SGZ axis is directed toward the supergalactic north pole (SGB = 90°) and the SGX and SGY axes lie in the supergalactic plane. Take the SGX axis to be directed toward an intersection of the Galactic and supergalactic plane (SGL = 0°, SGB = 0°) and it follows that the SGY axis is directed roughly 6° from the North Galactic Pole (SGL = 90°, SGB = 0°). Distances are derived from redshifts assuming $H_0 = 75\ h_{75}$ km s^{-1} Mpc^{-1}. Relativistic corrections are small, but, to be precise, luminosity distances are presented.

[2] Some minor fine-tuning of the supergalactic equator was attempted. There was optimum concentration to the plane after clockwise rotations of the coordinate system by 3° about each of the SGX and SGY axes

[3] The sample consists of 2371 galaxies with systemic velocities less than 3000 km s^{-1}. There is reasonable uniformity in coverage of the entire sky, though the effects of obscuration are severe for $|b| < 20°$. The sample will be described by Tully and Fisher (1986).

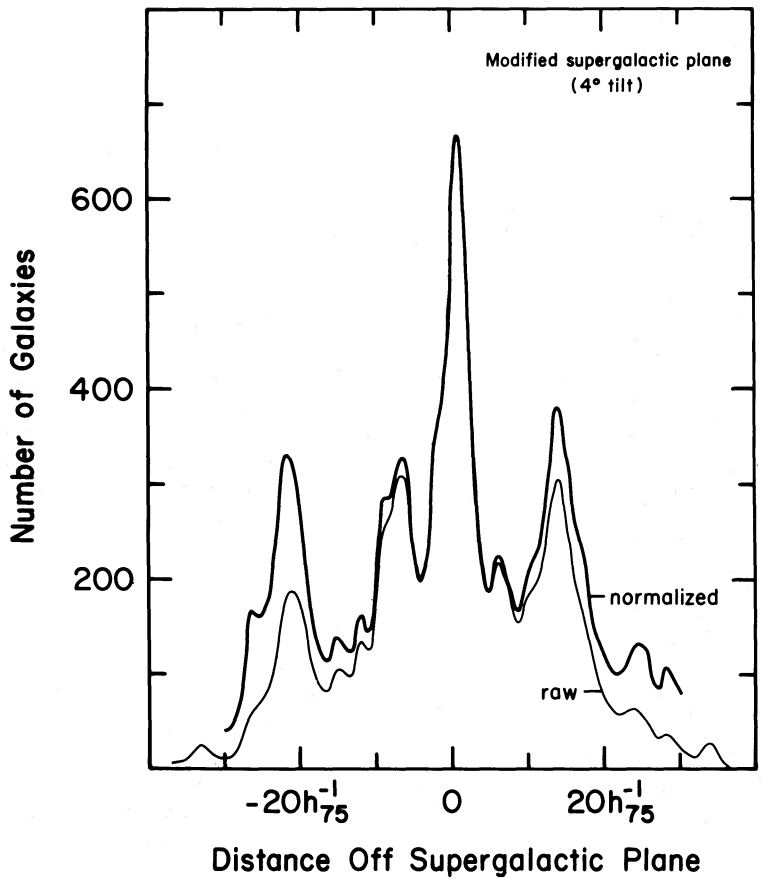

FIG. 1.—Distribution of nearby galaxies vertical to the plane of the Local Supercluster. The pole of the assumed plane has been tilted 4°.2 from the traditional pole. The thin curve gives raw galaxy counts in planes parallel to the assumed plane of the supercluster (0.5 h_{75}^{-1} Mpc bins). The heavy curve gives counts normalized by the fraction of unobscured area of a plane within the bounds of the sample to the unobscured area of the central plane.

5371 Cloud and the Grus Cloud, the SGZ dimensions are comparable with dimensions on other axes.

Figure 2*a* provides some support for this contention that there is stratification. A slab within the sample volume with $10 < \mathrm{SGY} < 30$ h_{75}^{-1} Mpc is considered, and the surface density projection onto the SGX-SGZ plane is shown (actually, the projection is onto the slightly modified plane described in footnote 2). This slab contains (from top to bottom) the Virgo III Cloud and most of the NGC 5371 Cloud, then much of the principal plane, then the Leo II-Crater layer (with the Centaurus Cluster), and, finally, the Antlia Cloud (with Hydra I).

Besides the stratified layers, Figure 2*a* shows that there are definite links between the conventional Local Supercluster and the Hydra-Centaurus region. Indeed, there is no clear demarcation of a separation between these entities, and viewers from afar might say that we live in the "Virgo-Hydra-Centaurus" Supercluster (Hydra I and Centaurus are barely closer to each other than either is to Virgo).

There is further evidence of stratification in the maps of the region between Virgo and Coma compiled by Tago, Einasto, and Saar (1984), based on Center for Astrophysics redshifts (Huchra *et al.* 1983). Figure 2*b* shows a composite of several maps from Tago *et al.* and a projected surface density map based on the data set associated with the *Atlas of Nearby Galaxies*. Two chains appear to link the Local and Coma Superclusters at very constant supergalactic latitudes. One is in the above-identified plane at $\mathrm{SGZ} = +13$ h_{75}^{-1} Mpc and the other is in the plane at $\mathrm{SGZ} = -8$ h_{75}^{-1} Mpc. These chains extend across the roughly 70 h_{75}^{-1} Mpc gap between the Virgo Cluster and Coma/Abell 1367.

There may be stratified structure on smaller scales. In the local neighborhood, the equatorial concentration is split into the Canes Venatici and Leo I/Leo Minor Clouds in distinct layers separated by about 3 h_{75}^{-1} Mpc in SGZ (Tully 1982).

In summary, the supergalactic coordinate system turns out to be a natural coordinate system for the display of almost all nearby features—not only the main plane that inspired the definition of the system. There is an apparent stratification in the distribution of nearby galaxies that may require a physical explanation. The local region will be described in greater detail in the *Atlas of Nearby Galaxies*. We turn now to consider evidence of structure on a parallel plane but on a much larger scale.

III. A VOLUME THAT INCLUDES THE COMA CLUSTER

As an intermediate step, I searched the literature for clusters within the distance of the Coma Cluster with velocity dispersions greater than 300 km s^{-1}, with the hope that such a sample would be reasonably complete. Thirty-seven such clusters were found. There were concentrations of clusters in the regions of Coma/A1367, Perseus-Pisces, and Hydra-Centaurus, and a couple of clusters in a poorly searched part of the southern celestial sky. All these regions turn out to be at

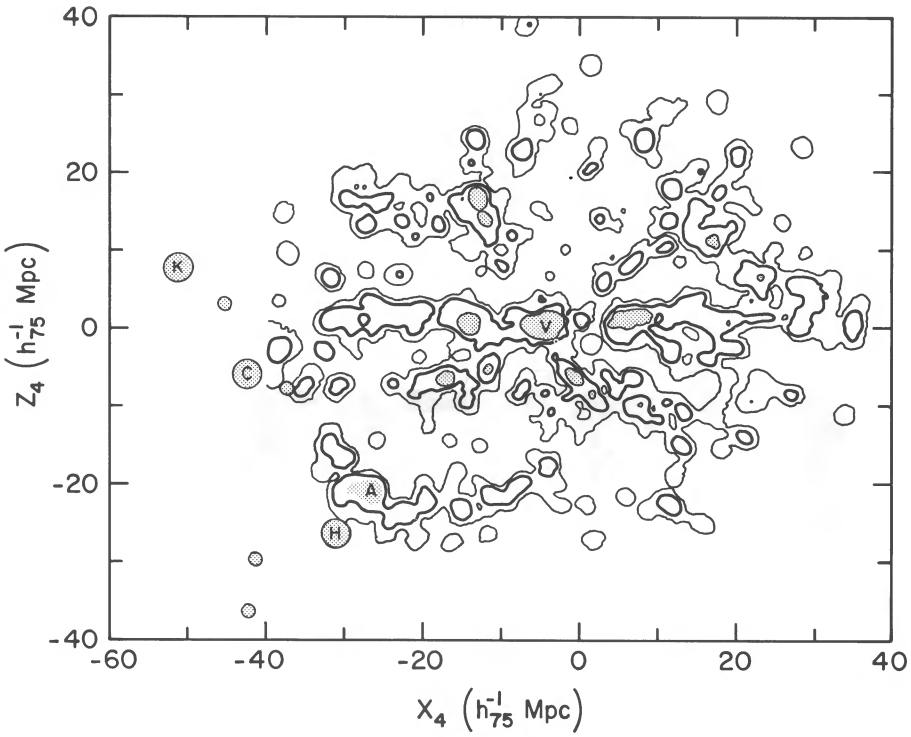

FIG. 2*a*

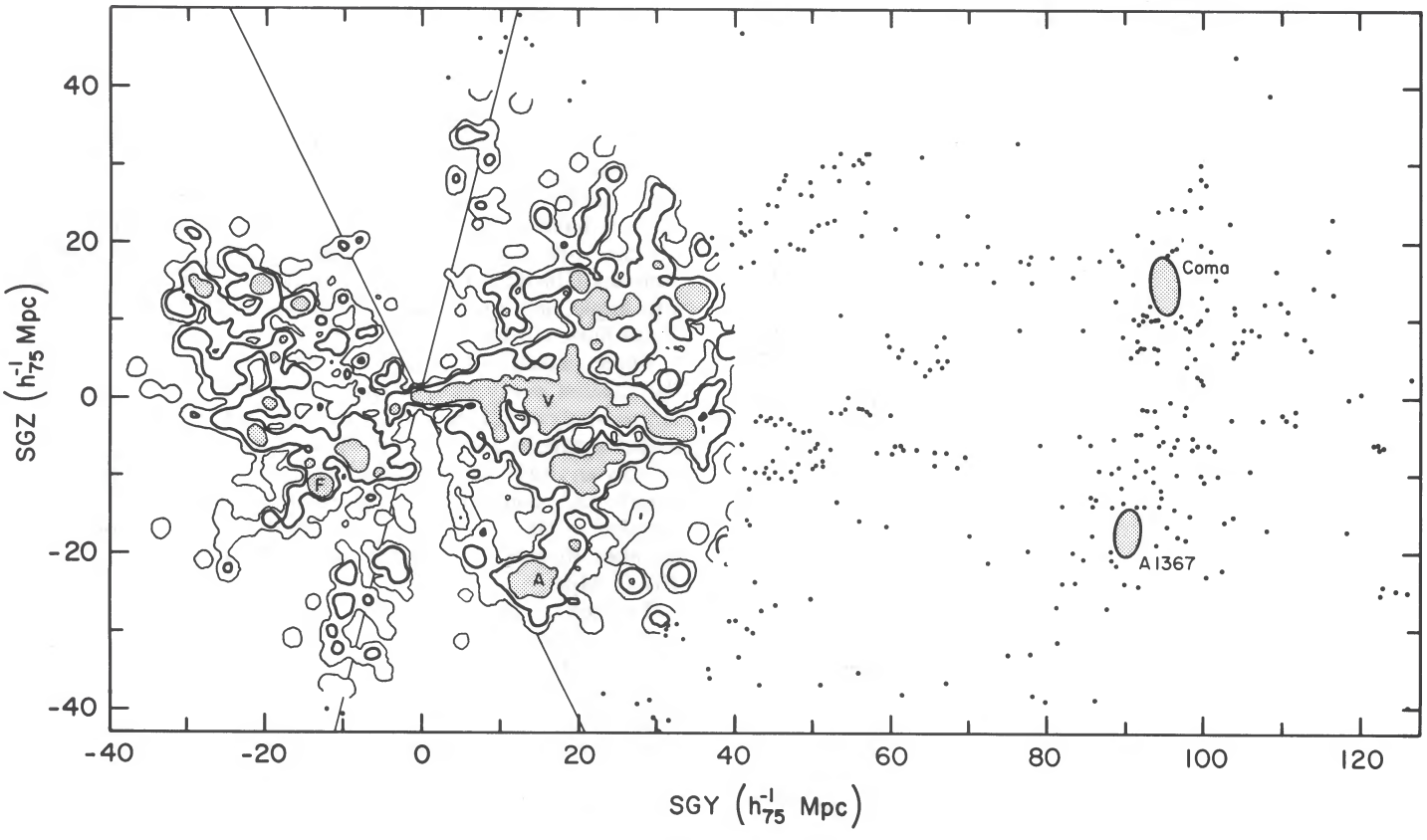

FIG. 2*b*

FIG. 2.—(*a*) Distribution of galaxies between Virgo and the Hydra-Centaurus Supercluster. A surface density map from the *Atlas of Nearby Galaxies* (Tully and Fisher 1986) is supplemented with data from Hopp and Materne (1985). Five clusters are identified: Virgo (V), Antlia (A), Hydra I (H), Centaurus (C), and Klemola 27 (K). Four minor groups identified by Hopp and Materne and outside my sample are located by small filled circles. The pole of the coordinate system has been tilted 4°.2 from the traditional supergalactic pole. (*b*) Distribution of galaxies between Virgo and the Coma/A1367 Supercluster. A surface density map from the *Atlas of Neaby Galaxies* is superposed on maps from Tago, Einasto, and Saar (1984). The surface density map is derived from a two-dimensional projection of all galaxies within a sphere of radius 40 h_{75}^{-1} Mpc of the Galaxy. Four Tago *et al.* maps with $|SGX| < 6.7\,h_{75}^{-1}$ Mpc have been combined to generate the outer area of the figure. The Tago *et al.* maps have been rescaled and morphological information has been suppressed. The $\pm 20°$ wedges identify the Galactic zone of avoidance. Three nearby clusters are located: Virgo (V), Fornax (F), and Antlia (A).

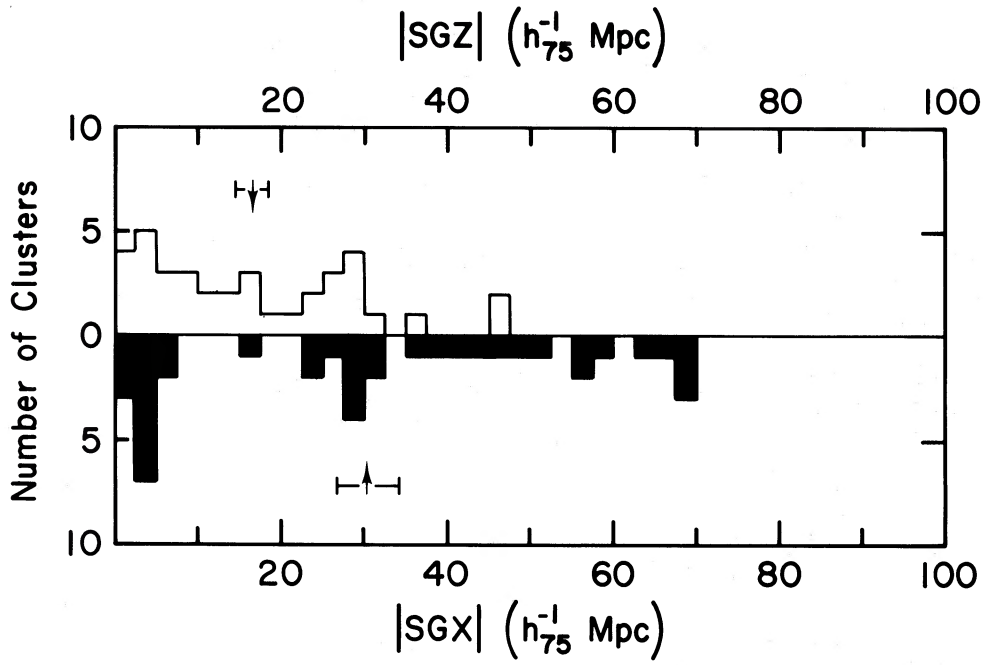

FIG. 3.—The distribution of 37 nearby clusters in |SGX| and |SGZ|. The sample consists of all clusters within the distance of the Coma Cluster identified to have a velocity dispersion greater than 300 km s^{-1}. The supergalactic equator lies in the SGX-SGY plane, while galactic obscuration lies within 6° of the SGX-SGZ plane. The occurrence of clusters at large values of SGX, but not SGZ, is evidence that the apparent flattening is not an artifact of obscuration. The difference in the mean values of |SGX| and |SGZ| has a significance of 3.2 σ.

low supergalactic latitudes. In a volume that extends out $95h_{75}^{-1}$ Mpc, all known clusters lie within $\pm 50\ h_{75}^{-1}$ Mpc of the supergalactic equator.

Figure 3 illustrates that the phenomenon is not a consequence of obscuration. The distribution of the clusters is shown as functions of the two Cartesian supergalactic coordinates SGX and SGZ, where the zone of obscuration is within 6° of the plane defined by these axes (i.e., obscuration should have similar effects along both these axes), and the equator of the Local Supercluster is in the SGX-SGY plane. Clusters have been found at low Galactic latitudes but only near the supergalactic equator. The supergalactic coordinate system, defined by the distribution of galaxies within $\sim 30\ h_{75}^{-1}$ Mpc, seems to have some relevance for clusters as far away as $100\ h_{75}^{-1}$ Mpc. Zel'dovich, Einasto, and Shandarin (1982) and Einasto *et al.* (1983) have noted the concentration of clusters toward the supergalactic plane in this domain.

IV. THE DISTRIBUTION OF CLUSTERS WITHIN 0.1c

a) The Sample

In an effort to see how far the apparently flattened distribution of clusters might extend, a sample of 214 clusters with measured redshifts less than 0.1c was accumulated. The Sarazin, Rood, and Struble (1982) tabulation of information on Abell (1958) clusters provides data on 182 clusters. Noonan (1981) provides data on 25 clusters south of declination −27°, the southern limit of the original Abell survey. In addition, the Virgo Cluster and six other northern clusters not cataloged by Abell but established to have velocity dispersions in excess of 500 km s^{-1} were included in the sample.

Almost certainly, this data set suffers from inhomogeneities with distance, between the north and south hemispheres, and as a function of Galactic latitude.

b) A Percolation Test

Bahcall and Soneira (1983) have demonstrated that there are strong two-point correlations between Abell clusters. Burns and Batuski (1984) provide a preliminary description of the three-dimensional distribution of these clusters. These latter authors have identified two great groupings of clusters within $z = 0.1$: one that envelops both the Hercules and Corona Borealis Clusters, and another that they call Pisces-Cetus. I will argue that we are an outlying member of a vast Pisces-Cetus Supercluster.

Three orthogonal projections illustrate the distribution of the clusters in my sample in Figure 4. The results of a percolation analysis (Einasto *et al.* 1984) are demonstrated by the coded symbols and contour lines. The percolation analysis groups any two clusters closer together than a specified scale length and, consequently, defines a network in which each member is closer than the scale length to at least one other member. Results are shown for percolation scales of 50, 60, and $70\ h_{75}^{-1}$ Mpc.

To keep the figure clear, only networks that grew to include at least 10 members are identified. With a percolation scale length of $50\ h_{75}^{-1}$ Mpc, only three structures had crossed the 10 member threshold. The two superclusters identified by Burns and Batuski (1984) are easily the largest: Hercules-Corona Borealis with 25 members (superclusters BS 12B, 13, 15, and 16 in the compilation by Bahcall and Soneira 1984) and Pisces-Cetus with 20 members (BS 1 and 2). Another entity that I will name the Sextans Supercluster has 14 members (BS 7).

If the percolation scale is increased to $60\ h_{75}^{-1}$ Mpc, there is a dramatic change. The Pisces-Cetus Supercluster grows to 48 members and now *includes the Virgo Cluster* (and now includes BS 10). The critical growth occurs as the percolation scale length transits the range 50–55 h_{75}^{-1} Mpc with the present sample. Four gaps are bridged: between the Pisces-Cetus core

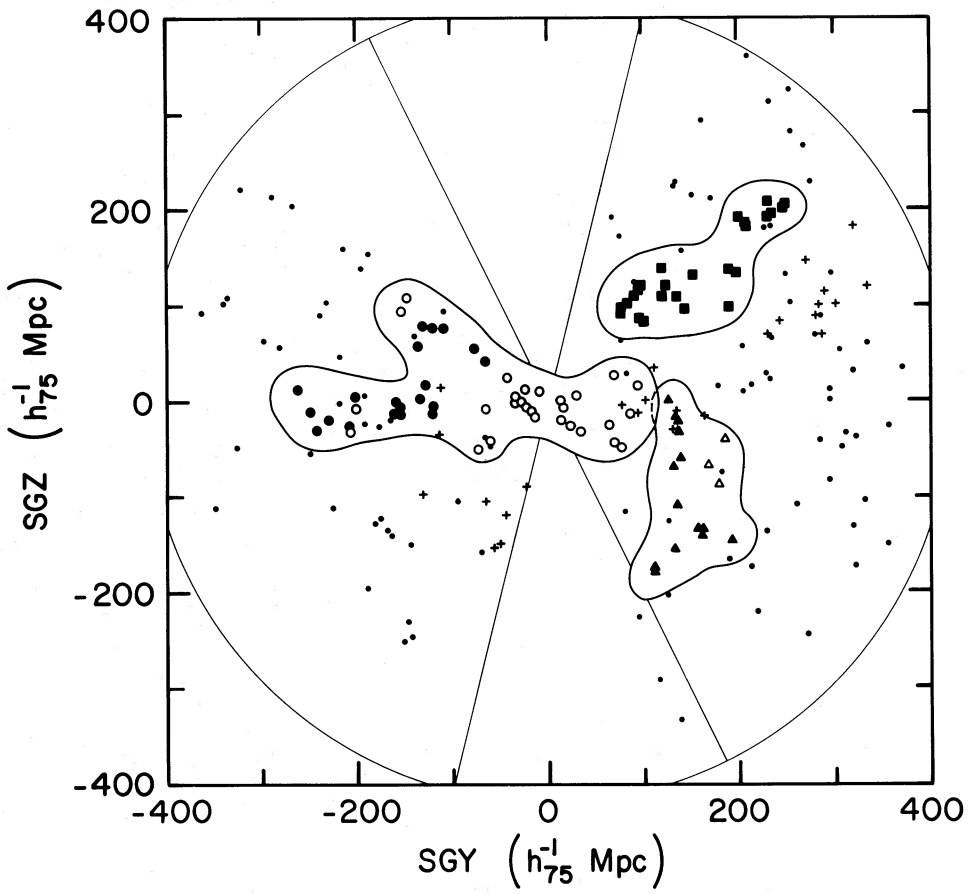

FIG. 4a

FIG. 4.—(*a*) The SGY-SGZ projection of 214 clusters with $z < 0.1$. With a percolation scale length of 50 h_{75}^{-1} Mpc, 25 clusters in Hercules-Corona Borealis are associated (*filled squares*), 20 clusters in Pisces-Cetus are associated (*filled circles*), and 14 clusters in Sextans are associated (*filled triangles*). With a percolation scale length of 60 h_{75}^{-1} Mpc, 28 additional clusters are associated with Pisces-Cetus (*open circles*) and three additional clusters are associated with Sextans (*open triangles*). Freehand contour lines enclose the three superclusters that are defined with this percolation scale length. With a percolation scale length of 70 h_{75}^{-1} Mpc, these three structures are linked and the clusters indicated by plusses have also been associated. The remaining unassociated clusters are located by small dots. The $\pm 20°$ zone of Galactic obscuration is indicated. (*b*) The SGX-SGZ projection of the same 214 clusters. Symbols have the same meaning as in (*a*). Galactic obscuration lies within 6° of the plane of this projection. (*c*) The SGX-SGY projection of the same 214 clusters. Symbols again have the same meaning. The zone of Galactic obscuration is indicated. This view is from the supergalactic pole. The small square at the origin indicates the dimensions of the traditional Local Supercluster.

and the Perseus-Pisces chain, across the zone of obscuration, on to Coma, and back to the Virgo Cluster and Hydra-Centaurus.

With a percolation scale of 60 h_{72}^{-1} Mpc, the Hercules and Sextans Superclusters have hardly grown. However, by a scale of 70 h_{75}^{-1} Mpc the three major units have coalesced. This one grand structure includes 115 clusters. The agglomeration that is defined by this percolation scale may not be physically significant since, as is seen in § V, at a characteristic distance of 200 h_{75}^{-1} Mpc the mean intercluster separation is $\sim 75\, h_{75}^{-1}$ Mpc with the present sample. It is noteworthy, though, that among the remaining 99 clusters in the sample there is no other percolation network with more than five members. As the percolation length increases further, more and more clusters are appended by the dominant network, but no other significant grouping is discerned. By a scale of 120 h_{75}^{-1} Mpc, 208 of 214 clusters have been united. The last cluster joins with a scale of 200 h_{75}^{-1} Mpc.

c) *The Morphology of the Pisces-Cetus Supercluster*

The striking aspect of the network that has percolated with a scale of 60 h_{75}^{-1} Mpc is its flattened nature (although there is one spur with eight of the 48 clusters that lies off the principal plane). It can be seen in Figure 4 that, if the spur of 8 clusters is ignored, this structure has the extreme dimensions $360 \times 200 \times 80\ h_{75}^{-1}$ Mpc (with the spur included, the extreme dimensions are $360 \times 240 \times 160\ h_{75}^{-1}$ Mpc). Remarkably, the plane defined by the long and intermediate dimensions *is coincident with the plane of the traditional Local Supercluster.* Without the spur, the difference in the orientation of the long axis with respect to the SGY axis is $1° \pm 5°$ (estimated uncertainty), and the difference in the orientation of the intermediate axis with respect to the SGX axis is $6° \pm 10°$ (est.).

The unexpected concentration of Abell-class clusters toward the supergalactic equator is illustrated directly in Figure 5, a histogram of the number of clusters as a function of SGZ. This plot is the analog for clusters of what was shown in Figure 1 for galaxies, except that the dimensions scale is amplified by a factor of 10. Again, there has been a normalization that accounts for the differences in unobscured area within planes at different distances off the supergalactic plane. Unlike before, no adjustments have been made for incompletion as a function of distance or declination.

The apparent flattened structure seen in Figure 4 is manifest-

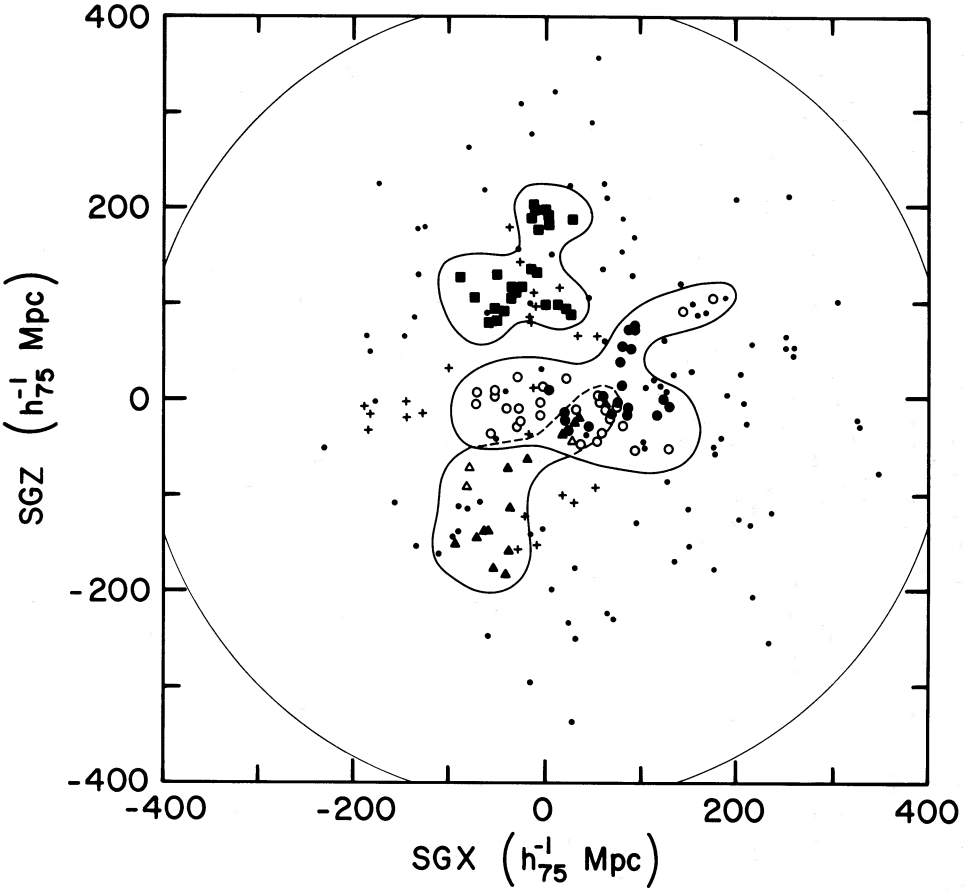

FIG. 4*b*

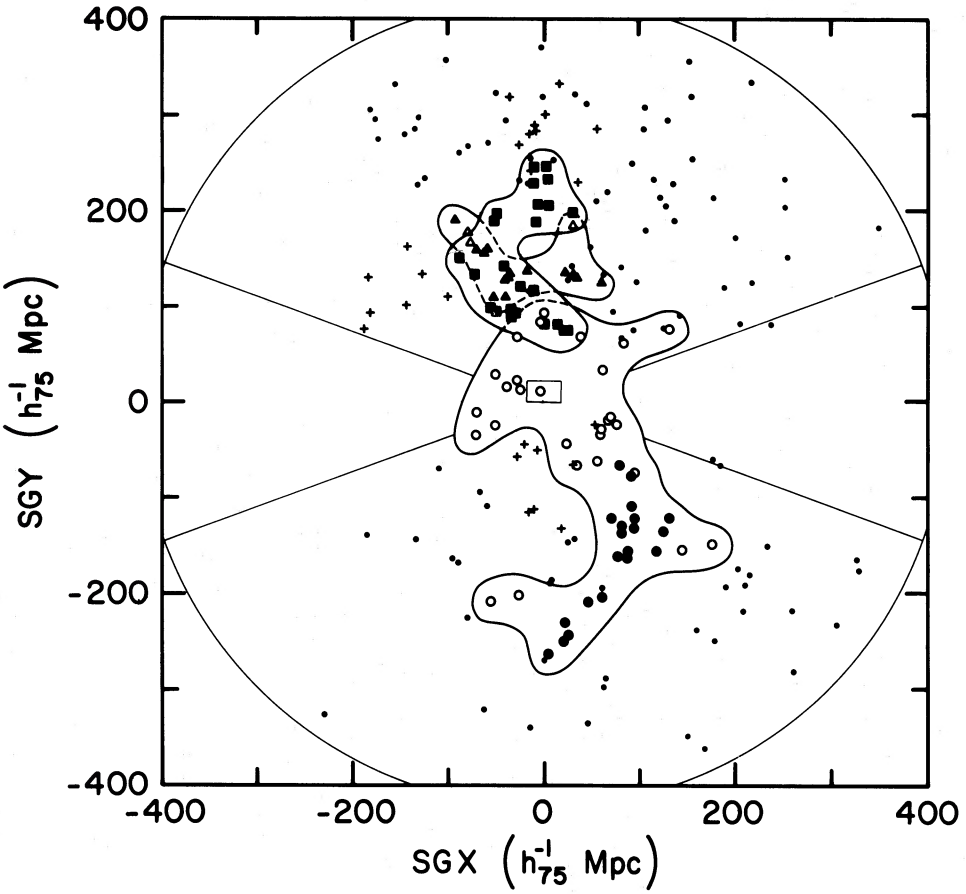

FIG. 4*c*

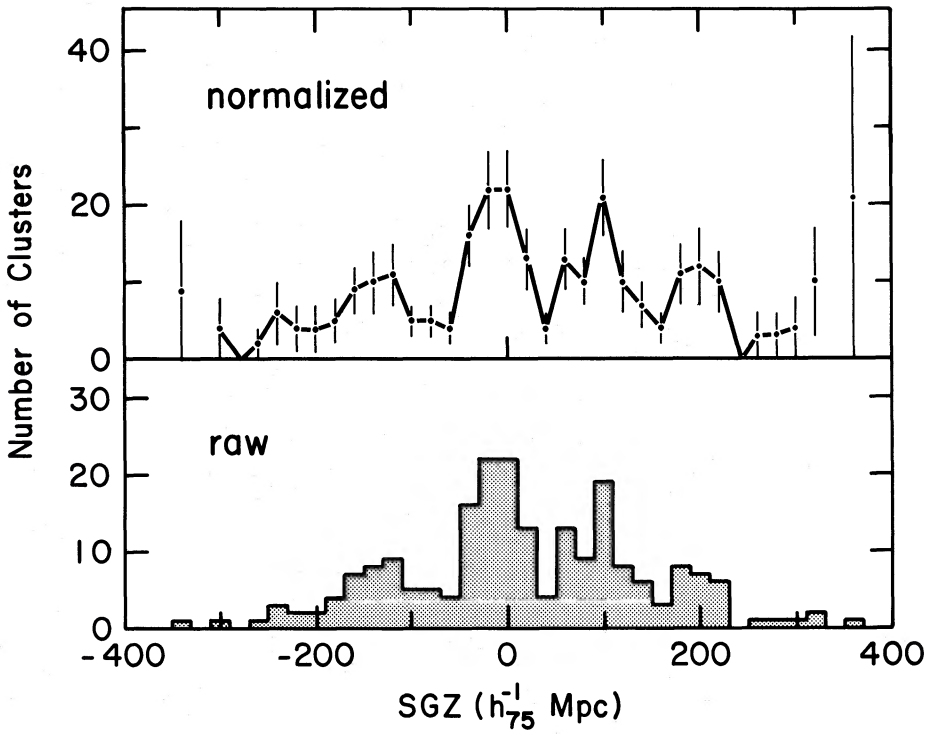

FIG. 5.—The distribution of the sample of 214 clusters as a function of distance from the supergalactic equator. The lower panel gives the distribution of the raw data. The upper panel has been normalized to account for differences in the unobscured area in planes as a function of supergalactic latitude. No corrections are made for incompleteness as a function of distance or declination.

ed in Figure 5 as a signal over four central bins, a width corresponding to 80 h_{75}^{-1} Mpc. There are 73 clusters in these bins rather than the 33 anticipated from the normalized plot, a 4.0 σ excess of 40 clusters.[4]

Batuski and Burns (1985) have recently discovered the existence of a filament in the distribution of Abell clusters that extends about 280 h_{75}^{-1} Mpc from the Perseus Cluster to the constellation Pegasus. This feature is the spur seen in Figure 4. It runs from Abell 426 at SGX = 70, SGY = −15, SGZ = −18 h_{75}^{-1} Mpc through Abell 2622 at SGX = 176, SGY = −148, SGZ = 106 h_{75}^{-1} Mpc and beyond, to Abell 2675 at SGX = 160, SGY = −239, SGZ = 89 h_{75}^{-1} Mpc. Batuski and Burns make a reasonably strong case for the existence of this filament, but the interesting thing about it is its great length, not its prominence as a haven for Abell clusters. The dominant nearby agglomeration of Abell clusters in the Southern Galactic Hemisphere is in Pisces-Cetus, as Burns and Batuski (1984) have noted.

d) Shectman's Sample

Just as the rest of the manuscript was completed, redshifts for a large sample of newly defined clusters were published by Shectman (1985). The region Shectman surveyed is centered on the Pisces-Cetus Supercluster and extends deep enough in redshift to provide good coverage of this feature. The new sample provides a fivefold increase in the number of clusters known within the limited region surveyed. However, the large structure that I have identified spills outside the bounds of the volume studied by Shectman. Consequently, this new sample is not appropriate for the delineation of the large-scale structure that is being discussed, but it does provide information on some internal details of the Pisces-Cetus agglomeration.

Between the new sample and the sample discussed previously, I have 111 clusters with $z < 0.1$ in the region studied by Shectman. Two orthogonal views of the distribution of these 111 clusters are given in Figure 6. Information regarding the results of a percolation analysis is communicated in the symbols.

The percolation test must suffer from boundary effects when applied to such a restricted volume. Nevertheless, the results provide a confirmation of the earlier analysis. There is little percolation on scales less than 20 h_{75}^{-1} Mpc. By 30 h_{75}^{-1} Mpc, two major units have percolated: 33 clusters in the core of Pisces-Cetus have merged, and there is an affiliation of 19 clusters to the foreground that includes members of the Perseus-Pisces Supercluster. By 35 h_{75}^{-1} Mpc, these two units have coalesced, and an additional 10 clusters in a spur south of the principal plane have been appended. This single entity contains 56% of the sample and is contained in a rectangular box that fills about 15% of the available volume. By a percolation scale length of 45 h_{75}^{-1} Mpc, 87 of the 111 clusters merge into the principal unit.

The new sample confirms the basic flattened nature and major axis dimension of the extended Pisces-Cetus Supercluster. However, some features are seen that were not apparent previously. Many clusters of galaxies are now seen in the vicinity of SGX ≈ 100, SGY ≈ −250, SGZ ≈ 0 h_{75}^{-1} Mpc. The spur south of the plane (open circles in Fig. 6) was not seen

[4] Since this article was completed, more cluster redshifts have been accumulated such that now a sample of 309 clusters exists (an augmentation of 44%). With the increased sample (Tully 1986), in the same 80 h_{75}^{-1} Mpc window there are 105 clusters, a 4.6 σ excess of 57 clusters over the expected number. With the new sample, even if all clusters within 100 h_{75}^{-1} Mpc are ignored (to crudely counteract the bias toward greater completion locally), there is still a 3.0 σ signal in the same 80 h_{75}^{-1} Mpc window.

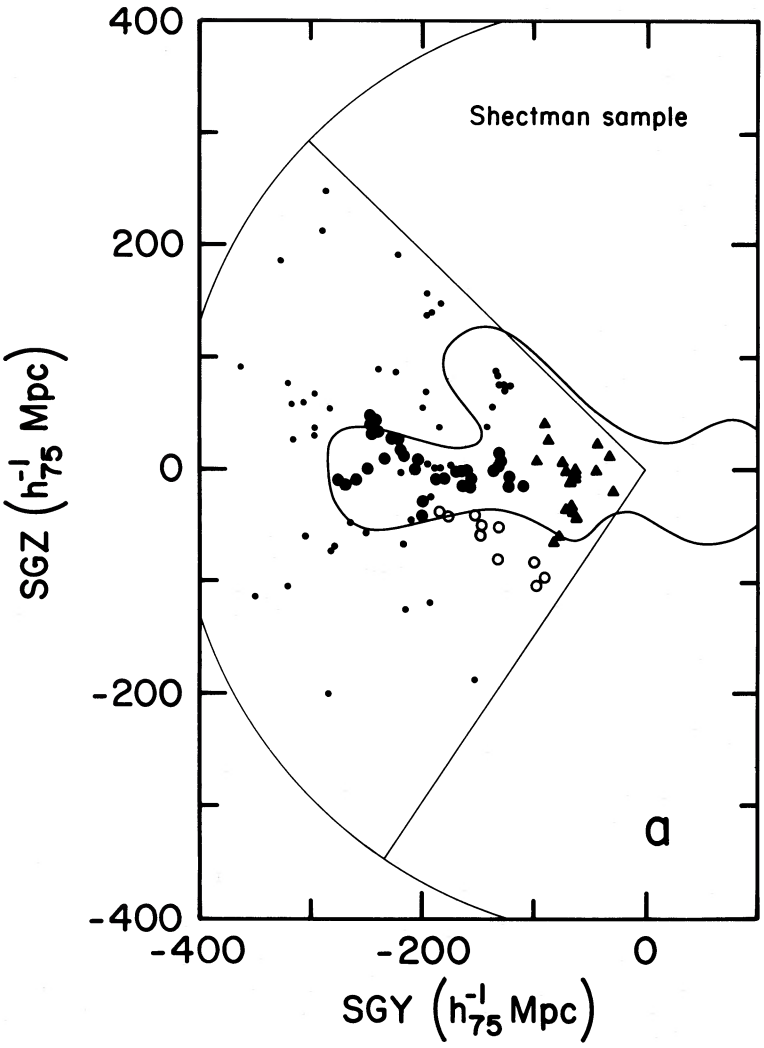

FIG. 6a

FIG. 6.—(*a*) The SGY-SGZ projection of 111 clusters in the region surveyed by Shectman (1985). Two separate networks within the extended Pisces-Cetus Supercluster are defined by a percolation scale length of 30 h_{75}^{-1} Mpc (*filled circles and triangles* respectively). These two entities are united with each other and with the spur south of the principal plane (*open circles*) with a percolation scale length of 35 h_{75}^{-1} Mpc. The sample limits of $b = -40$ and $z = 0.1$ are indicated. The outline of the structure identified in Fig. 4*a* is reproduced. (*b*) The SGX-SGY projection of the same 111 clusters. Symbols have the same meaning. The $\delta = -8$ limit is a plane that is skewed with respect to supergalactic coordinates, but the intersection of this plane with the supergalactic equator is indicated. The $b = -40$ and $z = 0.1$ limits are also shown. The outline of the structure identified in Fig. 4*c* is reproduced.

before. The spur north of the plane that was evident previously is seen only weakly here, because most of it lies at $b > -40$.

The distribution of the new sample with respect to the supergalactic plane is shown in Figure 7. Raw counts are given in Figure 7*a*, while normalized counts are given in Figure 7*b*. The normalization factor, shown in Figure 7*c*, depends on the relative area in planes at constant SGZ that lie within Shectman's window and $z < 0.1$. There is a significant enhancement of clusters centered on the supergalactic equator with FWHM of ~ 25 h_{75}^{-1} Mpc. The enhancement in the two central bins is 5–10 σ, depending on how the baseline is set. Once again, the supergalactic coordinate system is relevant to a sample at a large mean distance and one that is completely unrelated to the objects that defined the system.

V. HOLES AND HEDGES

Let us return to the all-sky sample of 214 clusters. If there is extensive clustering, then large holes can be expected. Indeed, they are there in the sample, if not in the universe. The question of the distribution of holes between clusters will only be considered in a preliminary fashion because there is too much uncertainty about the completeness of the sample.

Some idea about completeness can be gained from Figure 8, however. This plot shows the run of the number density of clusters with distance from us. Incompleteness must be a major cause of the fall-off with distance, although some contribution to the fall-off might result from looking outward from an overdense region.

Figure 9 shows that the size of the largest holes that can be found is a strong function of distance from us. That circumstance is expected from the fall-off in the density of known clusters demonstrated in Figure 8. The solid curve in Figure 9 indicates the expected increase in the maximum sizes of holes as a direct consequence of the decrease in density with the present sample, normalized to the case of a cubic lattice distribution.

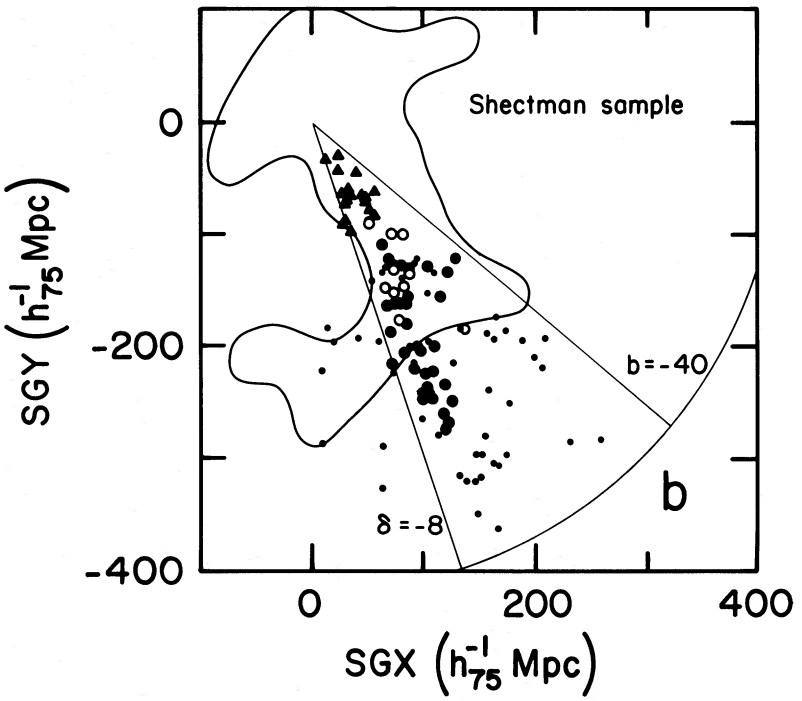

FIG. 6b

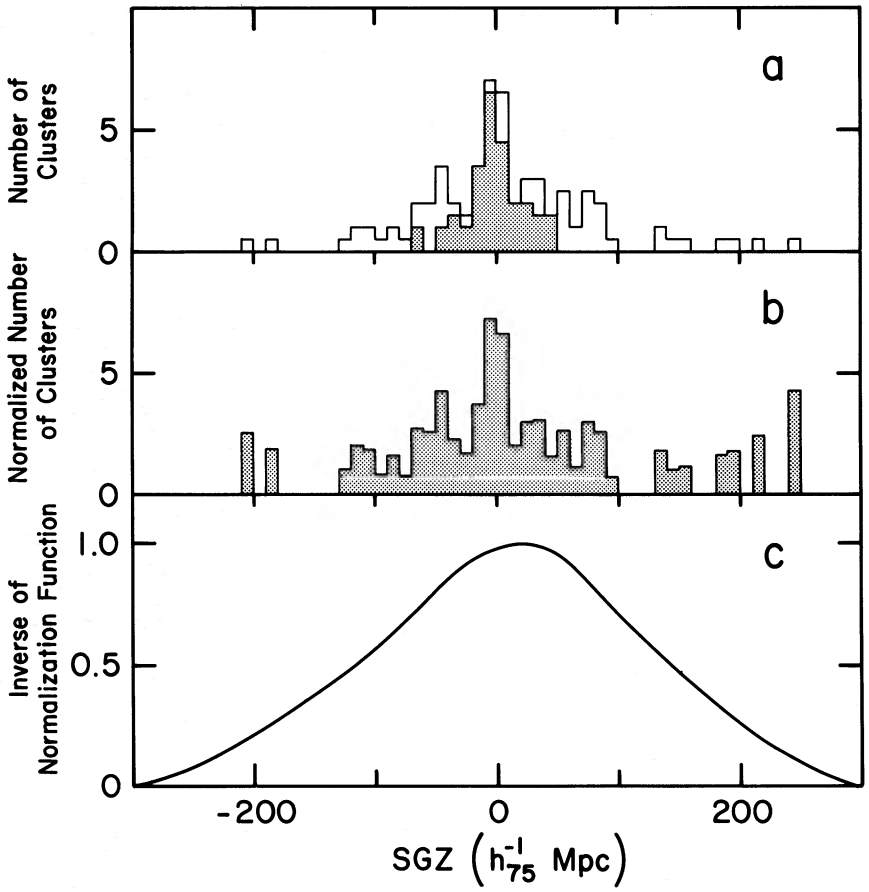

FIG. 7.—The distribution of clusters in the Shectman (1985) survey region as a function of distance from the supergalactic equator. (*a*) Raw data. The shaded portion represents clusters associated with the two major units that percolate with a scale of 30 h_{75}^{-1} Mpc. (*b*) The sample above has been normalized to account for the diminished area in planes at large |SGZ|. (*c*) The inverse of the normalization function: the relative area of planes normal to the SGZ axis in the Shectman sample region with $z < 0.1$.

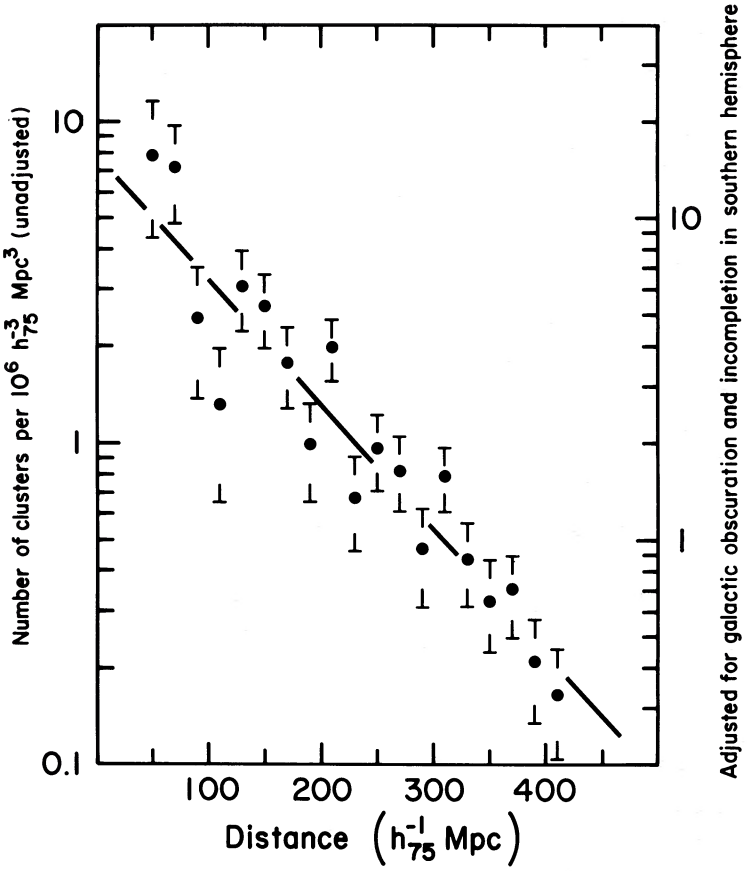

FIG. 8.—The density of clusters in the present sample as a function of distance. The left-hand scale gives raw densities in shells 20 h_{75}^{-1} Mpc thick, while the right-hand scale is adjusted by a factor of 2 to account in an approximate manner for obscuration and incompletion in the south celestial hemisphere. The straight line is a least squares single regression fit.

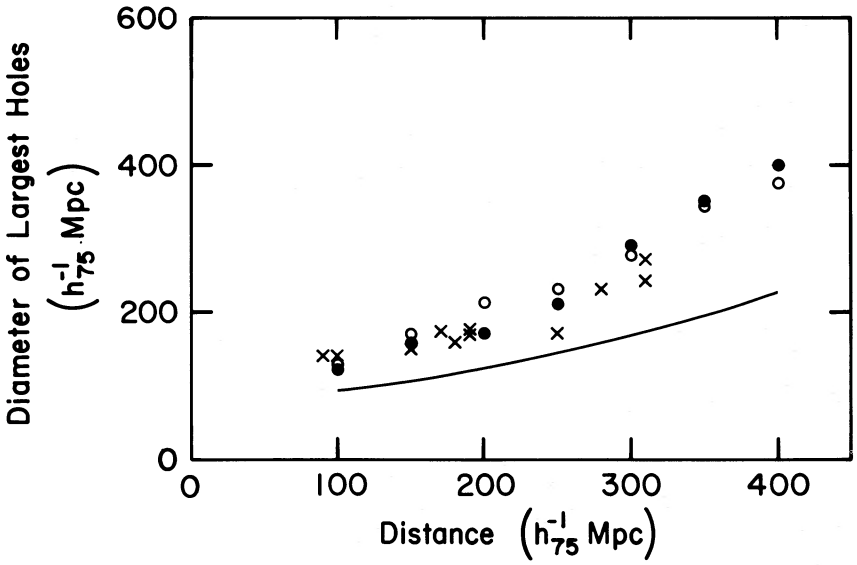

FIG. 9.—Diameters of the largest holes as a function of distance. *filled circles*, Northern Galactic Hemisphere; *open circles*, Southern Galactic Hemisphere; *crosses*, voids listed in Table 1. Essentially the entire Northern Galactic Hemisphere above $b = 30°$ was surveyed by Abell. The largest holes at adjacent sampling distances are correlated. The solid curve illustrates the largest holes that would exist if galaxies were distributed in a cubic lattice with the density dependence on distance given by the solid curve in Fig. 8.

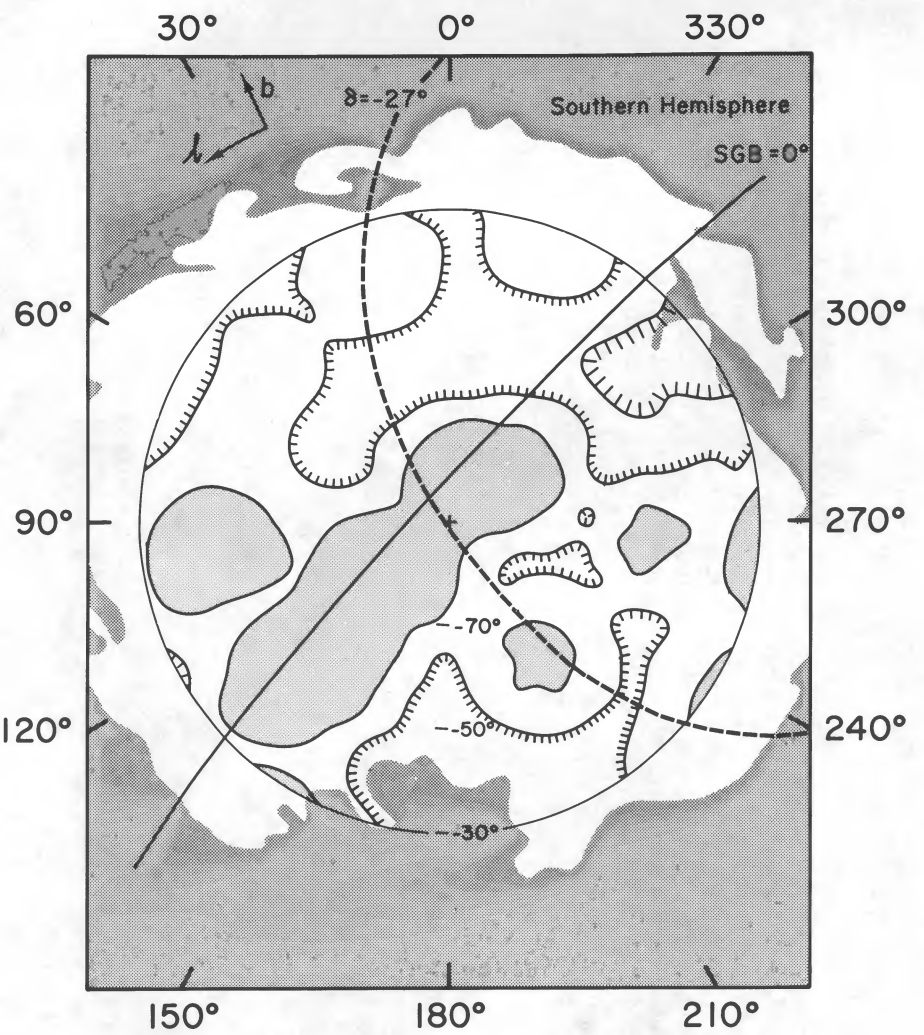

FIG. 10*a*

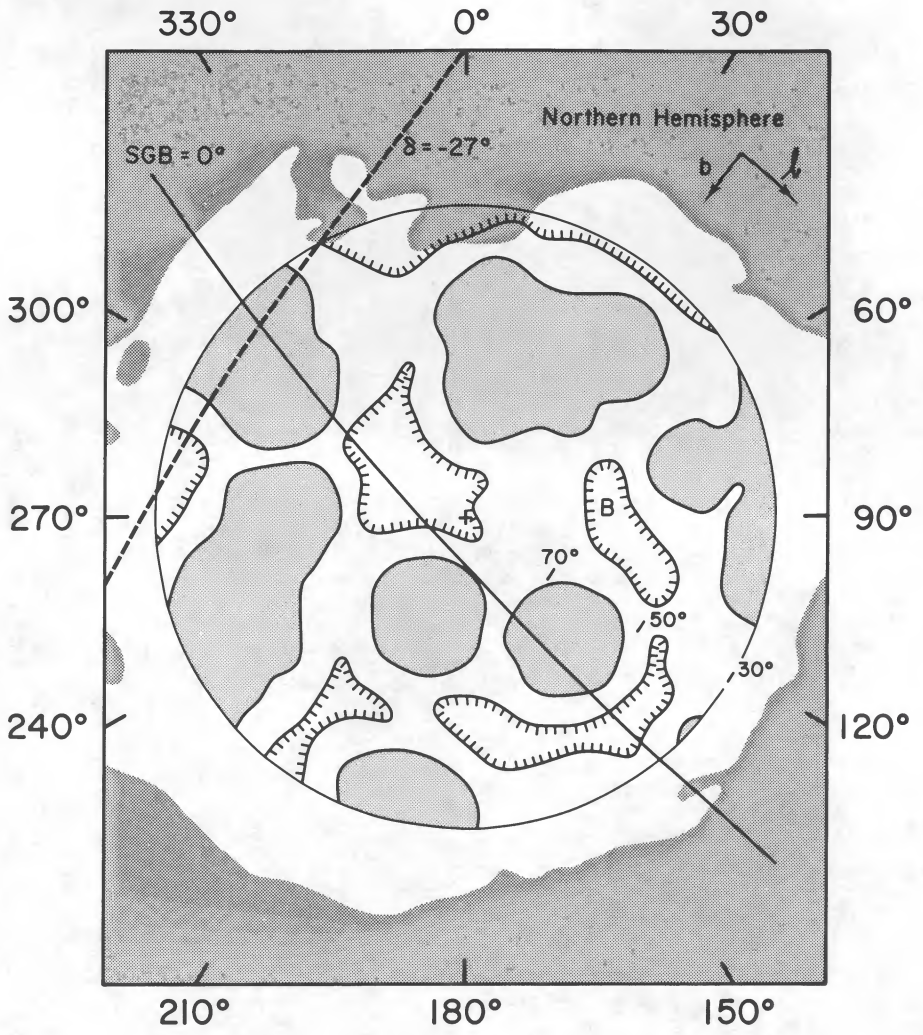

FIG. 10*b*

FIG. 10.—Holes between clusters at a distance of 200 h_{75}^{-1} Mpc. A grid of positions was considered at specified values of (l, b) and a distance of 200 h_{75}^{-1} Mpc. At each position, the sphere of the largest diameter was found that contained *no* cluster from the present sample. Contours of constant hole size on the grid are illustrated. Voids within the shaded contour have diameters less than 80 h_{75}^{-1} Mpc, while voids within the contours marked by short lines have diameters greater than 120 h_{75}^{-1} Mpc. In the Southern galactic hemisphere there is one additional contour where void diameters are greater than 180 h_{75}^{-1} Mpc. The search for holes was restricted to $|b| > 30$. The irregular shaded outer region is below the Burstein-Heiles H I contour corresponding to Galactic absorption of $A_B \approx 0.5$. The southern limit of the Abell survey, at $\delta = -27$, and the locus of the supergalactic equator, SGB = 0, are also indicated. (*a*) Northern Galactic Hemisphere. The void in Bootes discovered by Kirschner *et al.* (1981) is located at "B." (*b*) Southern Galactic Hemisphere. The major feature outlined by the 80 h_{75}^{-1} Mpc contour that is elongated parallel to the supergalactic equator is the core of the Pisces-Cetus Supercluster.

We see that it is possible to find arbitrarily large holes by looking out to distances with greater and greater incompleteness. By way of illustration, though, Figure 10 is a contour map of the distribution of holes that have centers in a shell of radius 200 h_{75}^{-1} Mpc. Additional information on the figure is the Burstein-Heiles (1982) H I contour that corresponds to $A_B \approx 0.5$ mag of obscuration, the southern limit to the Abell (1958) survey of $\delta = -27°$, and the supergalactic equator.

The largest spherical holes at a distance of 200 h_{75}^{-1} Mpc have diameters of ~ 200 h_{75}^{-1} Mpc. Some major holes might be attributed to incomplete sky coverage. However, there are some four voids in apparently well studied regions with diameters of 160–180 h_{75}^{-1} Mpc. One of these is the well-known void in Bootes (Kirshner *et al.* 1981), with a diameter of 160 h_{75}^{-1} Mpc. Table 1 gives the centers of the major apparent holes within a distance of 350 h_{75}^{-1} Mpc that lie in parts of the sky that should be well observed. The empty region with dimensions 400 × 200 h_{75}^{-1} Mpc identified by Bahcall and Soneira (1982) is not seen as one coherent entity in my analysis, but three of the voids listed in Table 1 lie in this space.

This section was included to serve three disparate purposes. (1) Figure 8 shows that there is a strong radial density gradient in the present sample, and that warns us to mistrust the percolation analysis except insofar as it helps locate major features. There are prospects that cluster samples will be significantly augmented soon so the reality of the suggested features can be tested. (2) The hole search algorithm is effective both for the location of voids and for the delineation of overdense regions. The gray region straddling the supergalactic equator in Figure 10*b* coincides with the Pisces-Cetus Supercluster. (3) Figure 10 provides a display that directly reveals where there may be dangers due to Galactic obscuration and incompleteness as a function of declination. Note that the feature in Pisces-Cetus is too thin perpendicular to the supergalactic equator to be an artifact caused by obscuration.

VI. DISCUSSION AND SUMMARY

1. Structure on very large scales and, specifically, the principal components of the nearest such structure have been recognized by most of the early workers in the field (cf. Shapley 1957; Abell 1961; Karachentsev 1966; de Vaucouleurs 1970; Shane 1975; Groth and Peebles 1977[5]). However, only crude distances could be estimated without redshifts. With knowledge of redshifts, Bahcall and Soneira (1983) have found strong correlations in the positions of clusters, and Bahcall and Soneira (1984) and Burns and Batuski (1984) have identified the major features of the cluster distribution.

It is suggested here for the first time that we are appended to one of these large-scale features. There is the obvious criticism to be made of the percolation analysis that greater completeness locally would favor percolation toward our position. At least, our perception of the extent and centroid of the Pisces-Cetus Supercluster must be biased in our direction. What makes the association of the local region with the structure in Pisces-Cetus rather compelling is the *combination* of (*a*) the results of the percolation analysis and (*b*) the parallel alignment of the several planes in the vicinity of the Virgo Cluster, the entire local region from Coma to Perseus-Pisces, and the overall Pisces-Cetus feature. Added evidence that we are part of a large-scale flattened structure is the links between Virgo, Coma/A1367, and Hydra-Centaurus seen in Figure 2 and the suggested extension of Perseus-Pisces through Lynx and Ursa Major toward Coma discussed by Giovanelli and Haynes (1982). From the Shectman (1985) sample, there is also a suggestion of a connection between the nearby Perseus-Pisces structure and the Pisces-Cetus region, where clusters with typical redshifts of 15,000 km s^{-1} are found to align so remarkably well along the supergalactic plane defined by galaxies in the vicinity of the Virgo Cluster.

2. What could cause the parallel alignment? The most natural explanation might be that local galaxies formed in clouds that had been distended by the gravitational influence of the extended Pisces-Cetus feature. The implication would be that the smaller structure did not form significantly in advance of the larger structure; i.e., there is a great deal of power on large scales.

If one either just sums the mass expected to exist in 48 rich clusters or calculates the mass within the entity outlined in Figure 4 in a universe with $0.1 < \Omega < 1$, then one concludes that there is 10^{17}–10^{18} $M_\odot$ associated with the local large-scale structure. Mass fluctuations on this scale, or only a little larger, would not have been inhibited from growth prior to recombination (cf. Jones 1976). If baryons were significantly clumped at recombination, however, there may be a conflict with the smoothness of the 3 K background radiation on both large and small scales (Wilson and Silk 1981; Silk and Wilson 1981; Uson and Wilkinson 1984).

Both the smoothness of the microwave background and the

[5] Groth and Peebles thought the large-scale fluctuations were probably an artifact of the observations.

TABLE 1

AN INCOMPLETE LIST OF VOIDS IN WELL-SURVEYED PARTS OF THE SKY
($\delta > -27°$, $|b| > 30°$, $A_B < 0^m.5$, distance < 350 h_{75}^{-1} Mpc)

Void Number	Distance (h_{75}^{-1} Mpc)	α(1950)	δ(1950)	l	b	SGL	SGB	Diameter (h_{75}^{-1} Mpc)	Note
1.....	90	17^h.0	+80°	110°	+30°	31°	+27°	140	1
2.....	100	21.0	−7	42	−30	262	+53	136	1
3.....	150	8.6	+13	214	+30	71	−51	150	1, 2
4.....	170	21.5	+5	59	−30	286	+52	173	1
5.....	180	14.3	+52	95	+60	66	+25	158	Bootes
6.....	190	23.0	−16	51	−63	272	+21	171	
7.....	190	12.8	+14	303	+76	104	+3	174	
8.....	250	10.0	+35	190	+54	67	−22	170	2
9.....	280	2.6	−11	185	−59	293	−28	229	
10.....	310	8.7	+58	158	+38	41	−12	243	2
11.....	310	16.8	+5	25	+30	129	+58	270	1

NOTES.—(1) Larger voids can be found at adjacent positions with lower $|b|$. (2) Within the region of the very large void claimed to exist by Bahcall and Soneira 1982.

implications concerning the power in fluctuations on large scales suggest that Abell clusters formed in biased locations, such that the observed enhancement of clusters in a region is not a fair reflection of the enhancement of total mass in the region. Kaiser (1984) has argued that the observed enhancement in the amplitude of the cluster-cluster correlation function over the galaxy-galaxy correlation function (Bahcall and Soneira 1983) could arise if rich clusters could only form upon exceeding a relatively high density threshold and, hence, were only likely to form in regions that are overdense on all relevant scales.

We can get a rough idea of the interplay between biasing requirements and constraints on the primordial fluctuation spectrum by considering specific models. The standard formulation of a power-law primordial spectrum is

$$\delta\rho/\rho \propto M^{-(n+3)/6} ,$$

where n is the exponent of the Fourier transform wavenumber: $|\delta_k|^2 = k^n$. We can infer that $\delta\rho/\rho \approx 1$ on scales of $10^{15}\ M_\odot$ today from the existence of collapsed objects on this scale. On one extreme, if there is no biased cluster formation, then the inference from the structure reported here that $\delta\rho/\rho \approx 1$ on scales of $10^{18}\ M_\odot$ would require $n \approx -3$. At another extreme, if the Zel'dovich spectrum is assumed (fluctuations enter the horizon with no characteristic mass scales), then $n = 1$ and the density fluctuations in clusters must represent an amplification of order 100 above the overall density fluctuations on a scale of $10^{18}\ M_\odot$. Such an amplification may seem extreme. A reasonable intermediate assumption would be that biasing is of order 10, as proposed by Kaiser (1984), and which seems to be the minimum required to accommodate the observed smoothness of the microwave background. A power law of index $n = -1$ or a cold dark matter spectrum of irregularities (Blumenthal *et al.* 1984) would just be acceptable.

One more comment regarding biased galaxy formation seems appropriate. On the one hand, biasing of order 10 or more seems to be required to reconcile the existence of clustering on a scale of $10^{18}\ M_\odot$ and the uniformity of the microwave background. On the other hand, in the context of Newtonian dynamics, the very flatness of the observed structure seems to imply a collapse time of order the age of the universe; i.e., no strong biasing. These observations might be taken as evidence for a non-Gaussian process (Peebles 1983), such as what could occur if there are "cosmic strings" (Vilenkin 1985; Albrecht, Brandenberger, and Turok 1985). Accordingly, clusters would not have formed as a consequence of collapse on large scales but would have formed due to local gravitational effects in the vicinity of defects that arose during a phase transition in the early universe.

3. Let me return to the apparent stratification of local structure into several parallel planes. It is to be appreciated that these are by no means filled planes. Galaxies are associated in clusters and filaments and, only occasionally, in two-dimensional features. There are three substantial clusters in the region described in the *Atlas of Nearby Galaxies*: Virgo, Fornax, and Antlia. Viewed from the supergalactic pole, the clouds of galaxies around these clusters appear to merge, but viewed from the equator, it is seen that these clouds *only rarely bridge the gaps between the stratification layers.* The two clusters just outside my survey volume, Hydra I and Centaurus, also appear to lie in layers defined locally, and it would be interesting to see whether or not galaxies in the vicinities of these clusters adhere to the same planes.

There are suggestive parallels between the observed stratified structure and certain N-body simulations that form multistream layers (Doroshkevich *et al.* 1980). It might be inferred that the local structure has had time to collapse and bounce in one dimension and there was little dissipation in the process.

On the one hand, I claim that there is stratification in planes parallel to the supergalactic equator over tens of megaparsecs and, on the other, all the well-known nearby structures globally intersect the equator at steep angles: the Coma /A1367 Supercluster (Gregory and Thompson 1978), the Perseus-Pisces Supercluster (Einasto, Jôeveer, and Saar 1980), and the Hydra-Centaurus Supercluster (Hopp and Materne 1985).

4. Finally, I am reminded of one other coincidence with the alignment of the plane of the supercluster around Virgo. Fliche and Souriau (1979) have claimed that there is a gap in the distribution of QSOs that becomes a flat plane with certain specific cosmological parameters ($\Lambda = 3.57H_0^2$ and a specified positive curvature term). The pole of that plane is coincident with the pole of the supergalactic coordinate system to within 28°. (Fliche and Souriau 1984 also claim that H I warps in nearby galaxies tend to align to the supergalactic plane.) I had viewed the coincidence of these two poles as an accident because the differences in scales were so great. Now that the dimensions associated with the Local Supercluster have grown by more than an order of magnitude in my eyes, a connection seems more plausible.

Thanks go to Laird Thompson and John Huchra for their comments on the manuscript. This research was supported by NSF grant AST 83-19951.

REFERENCES

Abell, G. O. 1958, *Ap. J. Suppl.*, **3**, 211.
———. 1961, *A.J.*, **66**, 607.
Albrecht, A., Brandenberger, R. H., and Turok, N. 1985, preprint.
Bahcall, N. A., and Soneira, R. M. 1982, *Ap. J.*, **262**, 419.
———. 1983, *Ap. J.*, **270**, 20.
———. 1984, *Ap. J.*, **277**, 27.
Batuski, D. J., and Burns, J. O. 1985, *Ap. J.*, **299**, 5.
Blumenthal, G. R., Faber, S. M., Primack, J. R., and Rees, M. J. 1984, *Nature*, **311**, 517.
Burns, J. O., and Batuski, D. J. 1984, in *Clusters and Groups of Galaxies*, ed. F. Mardirossian, G. Giuricin, and M. Mezzetti (Dordrecht: Reidel), p. 43.
Burstein, D., and Heiles, C. 1982, *A.J.*, **87**, 1165.
de Vaucouleurs, G. 1953, *A.J.*, **58**, 30.
———. 1956, *Vistas Astr.*, **2**, 1584.
———. 1970, *Science*, **167**, 1203.
———. 1975, *Ap. J.*, **202**, 610.
de Vaucouleurs, G., and de Vaucouleurs, A. 1964, *Reference Catalogue of Bright Galaxies* (Austin: University of Texas Press).
de Vaucouleurs, G., de Vaucouleurs, A., and Corwin, H. G., Jr. 1976, *Second Reference Catalogue of Bright Galaxies* (Austin: University of Texas Press).
Doroshkevich, A. G., Kotok, E. V., Novikov, I. D., Polyudov, A. N., Shandarin, S. F., and Sigov, Yu. S. 1980, *M.N.R.A.S.*, **192**, 321.
Einasto, J., Corwin, H. J., Jr., Huchra, J., Miller, R. H., and Tarenghi, M. 1983, *Highlights Astr.*, **6**, 757.
Einasto, J., Jôeveer, M., and Saar, E. 1980, *M.N.R.A.S.*, **193**, 353.
Einasto, J., Klypin, A. A., Saar, E., and Shandarin, S. F. 1984, *M.N.R.A.S.*, **206**, 529.
Fliche, H. H., and Souriau, J.-M. 1979, *Astr. Ap.*, **78**, 87.
———. 1984, in *Clusters and Groups of Galaxies*, ed. F. Mardirossian, G. Giurician, and M. Mezzetti (Dordrecht: Reidel), p. 77.
Giovanelli, R., and Haynes, M. P. 1982, *A.J.*, **87**, 1355.
Gregory, S. A., and Thompson, L. A. 1978, *Ap. J.*, **22**, 784.
Groth, E. J., and Peebles, P. J. E. 1977, *Ap. J.*, **217**, 385.
Hopp, U., and Materne, J. 1985, *Astr. Ap. Suppl.*, **61**, 93.
Huchra, J., Davis, M., Latham, D., and Tonry, J. 1983, *Ap. J. Suppl.*, **52**, 89.
Jones, B. J. T. 1976, *Rev. Mod. Phys.*, **48**, 107.

Kaiser, N. 1984, *Ap. J.* (*Letters*), **284**, L9.
Karachentsev, I. D. 1966, *Astrofizika*, **2**, 307 (English transl. in *Astrophysics*, **2**, 159).
Kirshner, R. P., Oemler, A., Jr., Schechter, P. L., and Shectman, S. A. 1981, *Ap. J.* (*Letters*), **248**, L57.
Noonan, T. W. 1981, *Ap. J. Suppl.*, **45**, 613.
Peebles, P. J. E. 1983, *Ap. J.*, **274**, 1.
Sarazin, C. L., Rood, H. J., and Struble, M. F. 1982, *Astr. Ap.*, **108**, L7.
Silk, J., and Wilson, M. L. 1981, *Ap. J.* (*Letters*), **244**, L37.
Shane, C. D. 1975, in *Stars and Stellar Systems*, Vol. **9**, *Galaxies and the Universe*, ed. A. Sandage, M. Sandage, and J. Kristian (Chicago: University of Chicago Press), p. 647.
Shapley, H. 1957, *The Inner Metagalaxy* (New Haven: Yale University Press).
Shectman, S. A. 1985, *Ap. J. Suppl.*, **57**, 77.
Tago, E., Einasto, J., and Saar, E. 1984, *M.N.R.A.S.*, **206**, 559.
Tully, R. B. 1982, *Ap. J.*, **257**, 389.
———. 1986, in *IAU Symposium 117, Dark Matter in the Universe*, ed. G. R. Knapp and J. Kormendy (Dordrecht: Reidel), in press.
Tully, R. B., and Fisher, J. R. 1986, *Atlas of Nearby Galaxies*, in preparation.
Uson, J. M., and Wilkinson, D. T. 1984, *Ap. J.* (*Letters*), **277**, L1.
Vilenkin, A. 1985, *Phys. Repts.*, **121**, 263.
Wilson, M. L., and Silk, J. 1981, *Ap. J.*, **243**, 14.
Zel'dovich, Ya. B., Einasto, J., and Shandarin, S. F. 1982, *Nature*, **300**, 407.

R. BRENT TULLY: Institute for Astronomy, 2680 Woodlawn Drive, Honolulu, HI 96822